Baptist Health South Florida

Scholarly Commons @ Baptist Health South Florida

All Publications

8-31-2023

Online adaptive radiotherapy: Assessment of planning technique and its impact on longitudinal plan quality robustness in pancreatic cancer

Kathryn Mittauer
Miami Cancer Institute, KathrynM@baptisthealth.net

Sreenija Yarlagadda
Miami Cancer Institute, Sreenija.Yarlagadda@baptisthealth.net

John Bryant
Miami Cancer Institute, JohnB2@baptisthealth.net

Tino Romaguera
Miami Cancer Institute, AntinogenesR@baptisthealth.net

Andres Gomez
Miami Cancer Institute, AndresGome@baptisthealth.net

See next page for additional authors

Follow this and additional works at: https://scholarlycommons.baptisthealth.net/se-all-publications

Citation

Mittauer, K. E., Yarlagadda, S., Bryant, J. M., Bassiri, N., Romaguera, T., Gomez, A. G., Herrera, R., Kotecha, R., Mehta, M. P., Gutierrez, A. N., & Chuong, M. D. (2023). Online adaptive radiotherapy: Assessment of planning technique and its impact on longitudinal plan quality robustness in pancreatic cancer. *Radiotherapy and oncology : journal of the European Society for Therapeutic Radiology and Oncology*, *188*, 109869. https://doi.org/10.1016/j.radonc.2023.109869

This Article -- Open Access is brought to you for free and open access by Scholarly Commons @ Baptist Health South Florida. It has been accepted for inclusion in All Publications by an authorized administrator of Scholarly Commons @ Baptist Health South Florida. For more information, please contact Carrief@baptisthealth.net.

Authors
Kathryn Mittauer, Sreenija Yarlagadda, John Bryant, Tino Romaguera, Andres Gomez, Robert Herrera, Rupesh Kotecha, Minesh Mehta, Alonso Gutierrez, and Michael Chuong

This article -- open access is available at Scholarly Commons @ Baptist Health South Florida:
https://scholarlycommons.baptisthealth.net/se-all-publications/5127

Radiotherapy and Oncology 188 (2023) 109869

Contents lists available at ScienceDirect

Radiotherapy and Oncology

journal homepage: www.thegreenjournal.com

Original Article

Online adaptive radiotherapy: Assessment of planning technique and its impact on longitudinal plan quality robustness in pancreatic cancer ☆

Kathryn E Mittauer [a,b,*], Sreenija Yarlagadda [a], John M. Bryant [a,b], Nema Bassiri [a,b], Tino Romaguera [a,b], Andres G Gomez [a], Robert Herrera [a], Rupesh Kotecha [a,b], Minesh P Mehta [a,b], Alonso N Gutierrez [a,b,1], Michael D Chuong [a,b]

[a] Department of Radiation Oncology, Miami Cancer Institute, Baptist Health South Florida, Miami, FL 33176, USA; and [b] Herbert Wertheim College of Medicine, Florida International University, Miami, FL 33199, USA

ARTICLE INFO

Article history:
Received 14 July 2021
Received in revised form 14 July 2023
Accepted 22 August 2023
Available online 31 August 2023

Keywords:
Online adaptive radiotherapy
MR-guided radiotherapy
Pancreatic radiotherapy
SBRT

ABSTRACT

Background and Purpose: Planning on a static dataset that reflects the simulation day anatomy is routine for SBRT. We hypothesize the quality of on-table adaptive plans is similar to the baseline plan when delivering stereotactic MR-guided adaptive radiotherapy (SMART) for pancreatic cancer (PCa).

Materials and Methods: Sixty-seven inoperable PCa patients were prescribed 50 Gy/5-fraction SMART. Baseline planning included: 3–5 mm gastrointestinal (GI) PRV, 50 Gy optimization target (PTV_{opt}) based on GI PRV, conformality rings, and contracted GTV to guide the hotspot. For each adaptation, GI anatomy was re-contoured, followed by re-optimization. Plan quality was evaluated for target coverage (TC = PTV_{opt} $V_{100\%}$/volume), PTV $D_{90\%}$ and $D_{80\%}$, homogeneity index (HI = PTV_{opt} $D_{2\%}/D_{98\%}$), prescription isodose/target volume (PITV), low-dose conformity (D_{2cm} = maximum dose at 2 cm from PTV_{opt}/Rx dose), and gradient index ($R_{50\%}$=50% Rx isodose volume/PTV_{opt} volume). A novel global planning metric, termed the Pancreas Adaptive Radiotherapy Score (PARTS), was developed and implemented based on GI OAR sparing, PTV/GTV coverage, and conformality. Adaptive robustness (baseline to fraction 1) and stability (difference between two fractions with highest GI PRV variation) were quantified.

Results: OAR constraints were met on all baseline (n = 67) and adaptive (n = 318) plans. Coverage for baseline/adaptive plans was mean ± SD at 44.9 ± 5.8 Gy/44.3 ± 5.5 Gy (PTV $D_{80\%}$), 50.1 ± 4.2 Gy/49.1 ± 4.7 Gy (PTV_{opt} $D_{80\%}$), and 80%±18%/74%±18% (TC), respectively. Mean homogeneity and conformality for baseline/adaptive plans were 0.87 ± 0.25/0.81 ± 0.30 (PITV), 3.81 ± 1.87/3.87 ± 2.0 ($R_{50\%}$), 1.53 ± 0.23/1.55 ± 0.23 (HI), and 58%±7%/59%±7% (D_{2cm}), respectively. PARTS was found to be a sensitive metric due to its additive influence of geometry changes on PARTS' sub-metrics. There were no statistical differences ($p > 0.05$) for stability, except for PARTS ($p = 0.04$, median difference −0.6%). Statistical differences for robustness when significant were small for most metrics (<2.0% median). Median adaptive re-optimizations were 2.

Conclusion: We describe a 5-fraction ablative SMART planning approach for PCa that is robust and stable during on-table adaption, due to gradients controlled by a GI PRV technique and the use of rings. These findings are noteworthy given that daily interfraction anatomic GI OAR differences are routine, thus necessitating on-table adaptation. This work supports feasibility towards utilizing a patient-independent, template on-table adaptive approach.

© 2023 The Author(s). Published by Elsevier B.V. Radiotherapy and Oncology 188 (2023) 109869 This is an open access article under the CC BY-NC-ND license (http://creativecommons.org/licenses/by-nc-nd/4.0/).

☆ This work has been accepted as abstract form to the AAPM 2021 Annual meeting as an oral presentation.

* Corresponding author at: Miami Cancer Institute Department of Radiation Oncology, 8900 N Kendall Dr, Miami, FL 33176, USA.
E-mail addresses: kathrynm@baptisthealth.net (K.E Mittauer), sreenija.yarlagadda@baptisthealth.net (S. Yarlagadda), john.bryant@moffitt.org (J.M. Bryant), nema.bassirigharb@baptisthealth.net (N. Bassiri), AntinogenesR@baptisthealth.net (T. Romaguera), AndresGome@baptisthealth.net (A.G Gomez), RobertoHerr@baptisthealth.net (R. Herrera), RupeshK@baptisthealth.net (R. Kotecha), MineshM@baptisthealth.net (M.P Mehta), AlonsoG@baptisthealth.net (A.N Gutierrez), MichaelChu@baptisthealth.net (M.D Chuong).
[1] Author Responsible for Statistical Analysis: Department of Radiation Oncology Miami Cancer Institute 8900 N Kendall Dr., Miami FL 33176.

https://doi.org/10.1016/j.radonc.2023.109869
0167-8140/© 2023 The Author(s). Published by Elsevier B.V.
This is an open access article under the CC BY-NC-ND license (http://creativecommons.org/licenses/by-nc-nd/4.0/).

Downloaded for Anonymous User (n/a) at Baptist Health South Florida Inc from ClinicalKey.com by Elsevier on May 10, 2024. For personal use only. No other uses without permission. Copyright ©2024. Elsevier Inc. All rights reserved.

On-table adaptive radiotherapy (RT) is able to account for interfractional anatomic changes using treatment plan re-optimization based on the patient's anatomy of the day [1,2,3]. Daily on-table plan adaptation is completed within several minutes while the patient remains in the treatment position [4]. This is in stark contrast to offline adaptive workflows that require hours to days during which significant anatomic changes may occur that may ultimately negate the clinical relevance of the plan adaptation.

While daily on-table plan adaptation is rapid, original treatment plan development using the initial simulation anatomy is typically performed over several days. The original plan establishes the initial planning objectives for the on-table re-optimization, which should be robust enough to account for interfractional changes and efficiently achieve high quality adaptive plans.

The advantage of on-table plan adaptation also poses one of its biggest challenges. Gastrointestinal (GI) luminal organs at risk (OAR) are frequently in proximity to and sometimes abut gross disease, thus traditionally limiting the prescribed radiation dose in the pancreas. Dose escalation becomes even more challenging due to frequent interfractional GI OAR changes that decrease the applicability of the initial optimization objectives based upon static simulation anatomy that may not be relevant. While manual updates to the optimization objectives are achievable during on-table adaptive replanning, each iteration increases the time that the patient must remain in the treatment position, that in turn increases the potential of significant GI OAR intrafractional motion. Therefore, the expeditious development of high quality and robust on-table adaptive plans is of critical importance [5,6].

Based on early clinical results, dose escalation provided by daily adaptation in MR-guided radiotherapy (MRgRT) may prolong overall survival (OS) while infrequently causing significant toxicity for patients with inoperable pancreatic cancer (PCa) [7–10]. We previously published the first clinical experience of ablative stereotactic MR-guided adaptive radiation therapy (SMART) for inoperable PCa patients exclusively treated on an MR-Linac that demonstrated favorable early efficacy and safety [10].

Due to the high dose gradients of stereotactic body radiotherapy (SBRT) adjacent to neighboring radiosensitive GI OARs, SMART plans are characterized by plan quality metrics that define treatment goals of adequate target coverage while minimizing normal tissue dose [7,11]. Reports on dosimetric plan quality for adaptive RT are currently limited [11–13]. Bohoudi *et al.* first reported on the robustness of SMART with an artificial neural network strategy for the initial planning objectives combined partial segmentation of OARs [11]. The initial experience was limited to ten patients with a prescription of 40 Gy (total dose) and a $D_{1\%}$ of 50 Gy to the PTV on an MR-guided cobalt treatment system.

The purpose of this study is to characterize the robustness of a novel adaptive planning technique. To this end, we evaluated plan quality for the first 67 SMART PCa patients treated at our institution with an ablative dose of 50 Gy in 5 fractions, which is higher than traditional pancreatic SBRT [10]. As such, this is the first reporting of a planning technique where an initial plan is created based off a standardized system and is used as the baseline for adaptive planning. The proposed planning technique is designed to be robust and effective to expedite on-table adaptive planning and deliver high quality plans.

A secondary objective was to develop a plan quality metric for pancreas SMART. A plan quality score was implemented in the spirit of the practice of adaptive pancreas RT, which consisted of the maximum GI luminal OAR doses, intermediate dose conformality, and target coverage to define the adaptive plan quality. Through this evaluation, the quality and robustness of stereotactic MR-guided adaptive plans can be benchmarked.

Materials and methods

Overview of study

After obtaining institutional review board (IRB) approval, we retrospectively evaluated the plan quality metrics of the first 67 consecutively treated PCa patients treated with SMART at our institution who were prescribed 50 Gy in 5 fractions on a 0.35 T MR-Linac system. We compared the initial baseline plans created typically over 5 business days using the simulation anatomy to the daily on-table adaptive plans created within several minutes prior to treatment delivery.

The planning technique as described below was standardized and implemented on all patients for the baseline plans. Thus, the quality of the adaptive plans is a direct assessment of the robustness of this planning method against daily internal anatomy changes. Herein, we refer to "robustness" as a departure from historical 'robust' optimization/evaluation terminology, i.e., "a dose distribution that is suitable for all or the majority of the error scenarios considered by the posed as n-dimensional problems; for instance, n = 1 can take into account the set-up error, n = 2 the range uncertainty for protons, n = 3 the breathing phases of a 4DCT and n = 4 possible anatomical changes (such as cavity filling and tumour shrinkage) to reduce the need for re-planning" according to Hernandez *et al.* [14]. We herein refer to adaptive "robustness" as the capability to efficiently and dynamically adjust the dosimetric gradient in optimization to maintain a high plan quality using the initial (or variation of) optimization objectives created from the simulation baseline anatomy and applying to a unique/new anatomy of the day during on-table adaptation.

Simulation and segmentation

Patient simulation was performed in the supine position and included a planning 0.35 T breath hold MR scan (preferably 25 sec, although if not tolerated then 17 sec) acquired on the MRIdian Linac (ViewRay Inc., Denver, CO, USA), followed by a planning CT scan on a SOMATOM Definition Edge (Siemens Healthcare, Forchheim, Germany). No immobilization was used for simulation or treatment since continuous MR imaging was utilized for motion management. The preferred arm position was down at sides to improve patient comfort.

A balanced steady-state free precession (TrueFISP) sequence was used for both simulation and each fractional MR scan for patient localization and online adaptive re-planning. The field of view (FOV) was 45x45x24 cm^3 (1.6x1.6x3.0 mm^3 resolution) for the 17 sec TrueFISP MR scan and either 40x40x43 cm^3 (1.5x1.5x3.0 mm^3 resolution) or 54x47x43 cm^3 (1.5x1.5x3.0 mm^3 resolution) for the 25 sec TrueFISP MR scan. To optimize image quality, the highest voxel resolution with the FOV encompassing all of the patient's relevant anatomy was selected. Maximum spatial distortion has been previously characterized for the TrueFISP sequence and is < 2.0 mm within 17.5 cm of isocenter [15].

Segmentation was performed on the MR simulation scan by a radiation oncologist with expertise in treating PCa. The gross target volume (GTV) was defined as tumor and locoregional lymph nodes as visualized on diagnostic imaging and simulation CT and/or MR scans. The GTV was uniformly expanded by a 3 mm setup margin (SM) to create the planning target volume (PTV). As previously reported, our experience with pancreatic SMART evolved from treatment of gross disease to adopting routine use of elective nodal irradiation (ENI) [10]. Our recent practice has included a clinical target volume (CTV) for inclusion of elective nodal volumes encompassing the celiac axis and superior mesenteric artery.

Downloaded for Anonymous User (n/a) at Baptist Health South Florida Inc from ClinicalKey.com by Elsevier on May 10, 2024. For personal use only. No other uses without permission. Copyright ©2024. Elsevier Inc. All rights reserved.

Specifically, the union of the GTV and elective volumes were uniformly expanded 3 mm for the CTV delineation, then a 3 mm isotropic SM expansion was applied for the PTV creation. OARs delineated for all cases included the stomach, duodenum, small bowel, large bowel, kidneys, liver, and spinal cord.

Planning technique

Visual representation of the target optimization ROIs and respective dose gradients based on daily position of GI OARs is shown in Fig. 1. While the intent was to deliver at least the prescription dose of 50 Gy in 5 fractions to the entirety of the PTV, this was not feasible for most patients while also respecting OAR constraints, given the proximity of GI OARs. All plans used a respective 0.03 cc and 0.5 cc institutional GI OAR constraints in accordance to Chuong *et al.* [10]. Table A1 (Appendix) describes the OAR constraints used in this study. Of note, a range of OAR constraints are shown in Table A1, due to the enrollment of a subset of patients on clinical trials with differing constraints.

A GI planning organ at risk volume (PRV) was created as an optimization structure to define the dose fall off between the proximal GI OARs and the target. The PRV_{GI} (Fig. 1, Fig. 2**B**) was defined by a 3 mm or 5 mm isotopic expansion of the union of the stomach, duodenum, small bowel, and large bowel (i.e., $AllOAR_{GI}$) (Fig. 2**A**). Our early experience incorporated a 5 mm PRV_{GI} margin (initial 21/67 patients) although when it became apparent that this was very well-tolerated, our practice evolved to instead use a 3 mm PRV_{GI} margin (most recent 46/67 patients) with the intent of increasing the volume of the target receiving at least the prescription dose. To this end, for this study baseline plans were compared between a 3 mm and a 5 mm PRV_{GI} margin to quantify the impact of PRV_{GI} margin on plan quality using the Kolmogorov-Smirnov test.

The dose within the target volume was defined through three gradient levels based on proximity to the $AllOAR_{GI}$: 30 Gy, 50 Gy, and 60 Gy (Fig. 2**C**). Any overlapping portion of the GTV and PTV by the PRV_{GI} was optimized to achieve 25–35 Gy. The non-overlapping portion of the GTV and PTV with the PRV_{GI} was defined as GTV_{opt} and PTV_{opt}, respectively, (Fig. 1**,** Fig. 2**B**) and optimized to achieve at least 50 Gy (Fig. 2**C**). To drive the placement of the hot-spot in a favorable location central to the GTV and away from the GI interface, a 3–5 mm contraction of the GTV_{opt} was performed and denoted as GTV_{core}. The GTV_{core} was intended to receive at least 120% (i.e., 60 Gy) of the prescription dose with maximum point dose of 135%-140% (Fig. 2**C**). To enable updating of the optimization ROIs based on daily changes of GI OARs and/or deformation changes of target volumes, predefined logic rules were inputted into the MRIdian treatment planning system (TPS) that included Boolean operation of $AllOAR_{GI}$, margin expansion for PRV_{GI}, Boolean operations of PTV_{opt} and GTV_{opt}, and margin contraction of GTV_{core}.

To control the dose conformality of the plan, two ring approaches were utilized in our planning technique. A 1 cm thick shell, denoted as $Ring_{2cm}$, encompassed a 2–3 cm expansion from the surface of PTV_{opt}, and was used to contain high dose spillage to the 50% isodose line (i.e., 25 Gy) (Fig. 1**,** Fig. 2). An additional ring defined as $Ring_{LowDose}$ was used to control the low dose conformality and expanded 3 cm from the surface of PTV_{opt} to the external of the patient (Fig. 1**,** Fig. 2). An additional non-planning-based ring was created for delineation of OARs to edit on daily basis for online adaptive RT. This contouring ring denoted as *AdaptiveContouring* was a non-uniform expansion of PTV_{opt}: 3 cm radially and 2 cm cranial/caudal. All expansions, contractions, and Boolean operations were setup as predefined rules in the MRIdian TPS to enable efficient application of the contour propagation for daily adaptation.

Treatment plans were 6 MV, flattening-filter free, step-and-shoot IMRT with beam angles isotropic around the patient with

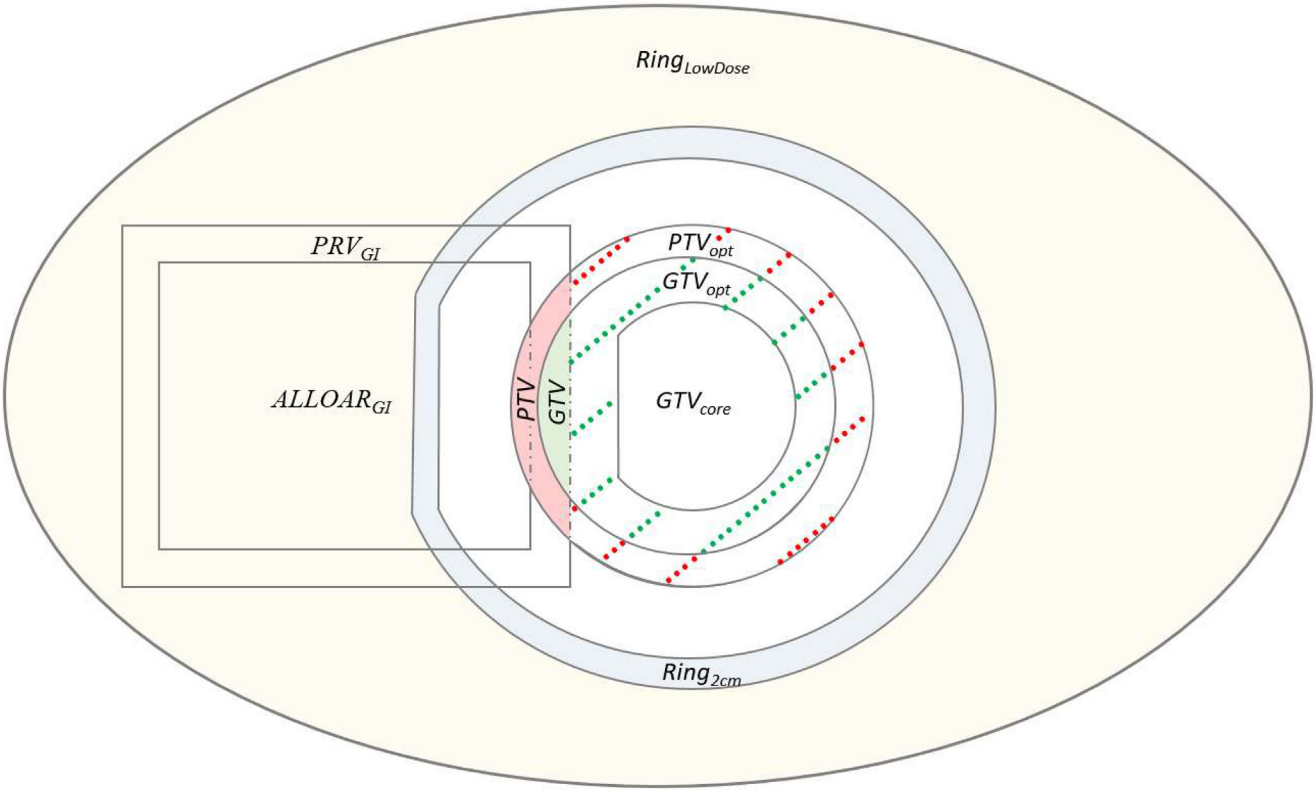

Fig. 1. Visual representation of planning technique to create overlapping and non-overlapping optimization structures for defining target dose volumes of 30 Gy, 50 Gy, and 60 Gy based on the daily position of gastrointestinal organs at risk.

Downloaded for Anonymous User (n/a) at Baptist Health South Florida Inc from ClinicalKey.com by Elsevier on May 10, 2024. For personal use only. No other uses without permission. Copyright ©2024. Elsevier Inc. All rights reserved.

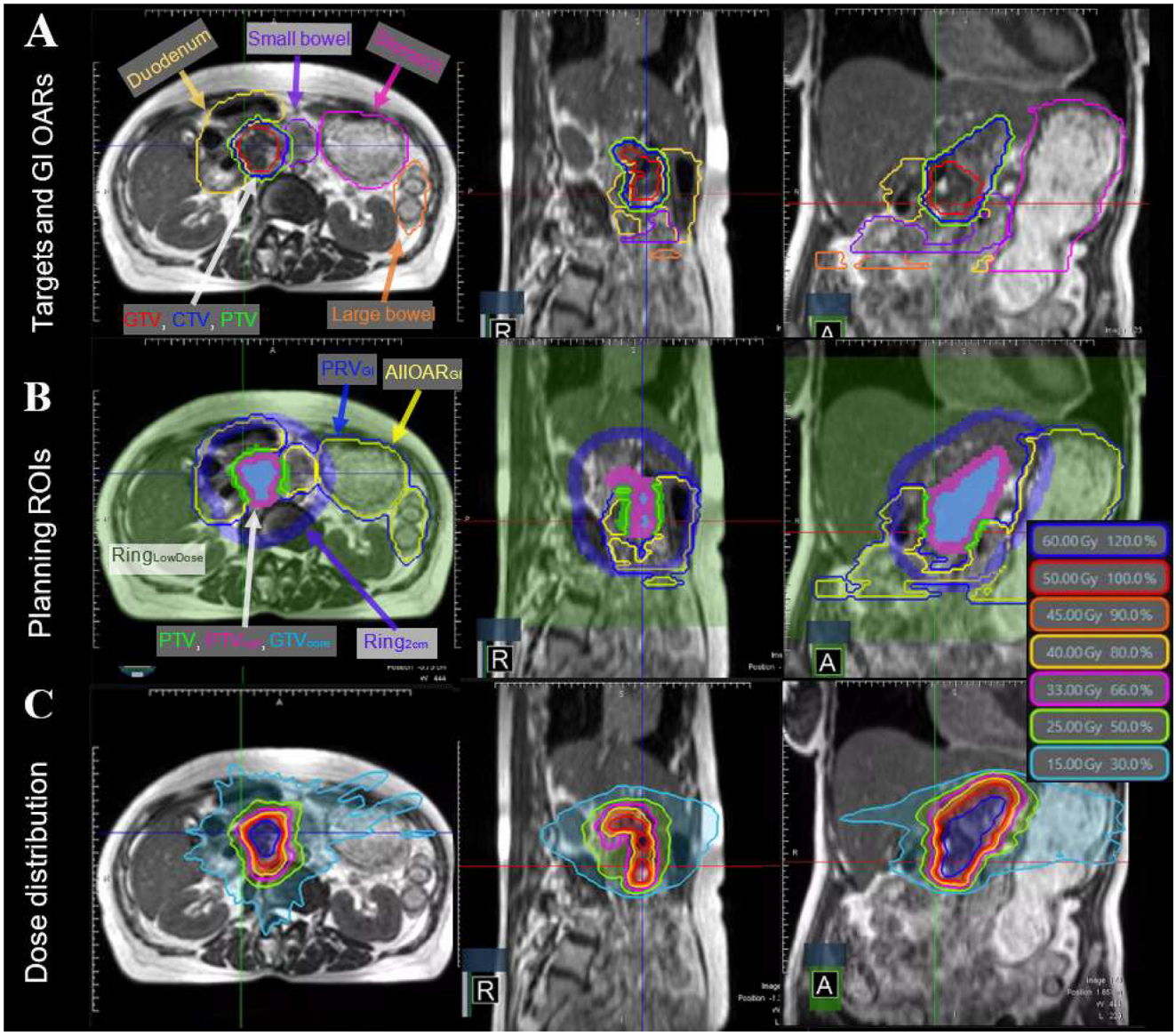

Fig. 2. 3D MR scan showing GTV, CTV, and PTV with relevant GI OARs (Fig. 2A), 3D MR scan showing optimization ROIs of $AllOAR_{GI}$, PRV_{GI}, PTV, PTV_{opt} GTV_{opt}, $Ring_{2cm}$, $Ring_{LowDose}$ (Fig. 2B), and 3D MR scan with optimization ROIs and isodose lines (Fig. 2C).

avoidance 2 cm from intersection at the patient arms and couch edges. Beam arrangement of early plans typically included 12–15 beams (32 patients). We transitioned to planning with 16–21 beams (35 patients), to enable greater degrees of freedom to accommodate the daily anatomical variations, since adding or changing the beam orientation is not feasible in the adaptive workflow [16]. Baseline plans were compared between beam arrangements of 12–15 beams and 16–21 beams to quantify the impact of beam numbers on plan quality for this study using the Kolmogorov-Smirnov test. Plan optimization was performed with a 2–3 mm^3 bixel and included optimization objectives of PTV, PTV_{opt}, GTV_{core}, $Ring_{2cm}$, $Ring_{LowDose}$, stomach, small bowel, large bowel, kidneys, spinal cord, and cauda equina. Delivery time was driven by the number of segments on the initial baseline plans with plans starting at 50 segments. The ungated total delivery time (i.e., beam-on time, MLC and gantry motion time) was set generally below 10 minutes, with some exceptions being above 10 minutes if additional modulation (i.e., higher number of segments) was warranted. Monte Carlo dose calculation with magnetic field corrections was performed with a 2 mm^3 dose grid resolution and 1% statistical uncertainty.

For propagation of electron density to the MR scan, two electron density approaches were utilized: (1) bulk density assignment and (2) deformed CT to the MR frame of reference. For the deformed CT approach, the CT simulation scan was deformed to the MR simulation scan with manual edits of air and tissue override as needed [17]. For the bulk density approach, density assignments included vertebral bodies as bone, external as water, and any abdominal gas as air. The deformed CT approach was previously used and evolved to the bulk approach due to efficiency gains during online adaptive workflow per institutional guidelines [18].

On-table adaptive replanning

The on-table adaptive MRgRT workflow has been previously reported [10,17]. Target volumes were rigidly registered from the simulation MR to the daily volumetric MR scan frame of reference and OARs were deformably registered. As previously described, all

Downloaded for Anonymous User (n/a) at Baptist Health South Florida Inc from ClinicalKey.com by Elsevier on May 10, 2024. For personal use only. No other uses without permission. Copyright ©2024. Elsevier Inc. All rights reserved.

OARs within the 2–3 cm asymmetric *AdaptiveContouring* ring were reviewed and manually edited as necessary. Targets were manually edited for any rotation and/or deformation.

Following segmentation, prediction of target and OAR dosimetry of the initial plan on the current anatomy and contours (i.e., predicted dose) was performed. The same planning criteria used for the initial plan were applied to the on-table adaptive planning process. Adaptive plan optimization was performed to meet dose constraints and/or improve target coverage. After the first optimization, further re-optimization was performed as necessary through adjustments to the cost function of the relevant ROIs, (i.e., manually editing power, importance, and/or dose threshold of optimization objective). If all constraints were met based on the predicted dose and the target coverage was not improved for the re-optimized plan beyond the statistical noise of the Monte Carlo dose calculation, then the baseline plan was used for treatment. The first priority was to ensure that OAR constraints were met, and secondarily to optimize high target coverage.

Plan quality assessment

For all 67 patients, a retrospective analysis was performed between the plan quality of the initial baseline plan and adaptive plans across all 5 on-table adaptive fractions. To quantify the quality robustness of online adaptive plans, the difference in plan quality metrics between the fraction 1 adaptive plan and the baseline plan was evaluated. A paired Wilcoxon-signed rank test was used to account for non-normal distributions.

To quantify the stability of the online adaptive planning quality, metrics were compared between the two adaptive fractions with the smallest and largest variance in overlapping GI OARs using a ratio of PTV_{opt}/PTV. Here, a PTV_{opt}/PTV of 1 indicates no overlap of PRV_{GI} with PTV, while a value of 0 indicates complete overlap. Similarly, a paired Wilcoxon-signed rank test was used for statistical analysis. Statistical significance in difference was assumed to be $p < 0.05$ for all evaluations.

Since the GI luminal OAR constraints were met on all adaptive plans and baseline plans, we did not compare GI luminal doses between these groups. Instead, we evaluated the plan quality differences to the GI luminal OARs between the adaptive dose and predicted dose (i.e., initial plan recalculated on fractional MR anatomy of day) as an assessment of the indication of adaptation for our isotoxicity approach. Specifically, we evaluated the volume receiving 35 Gy ($V_{35\ Gy}$) for stomach, duodenum, and small bowel and the volume receiving 38 Gy ($V_{38\ Gy}$) for large bowel.

Plan quality metrics were used to evaluate dose conformality included: homogeneity index (HI = PTV_{opt} $D_{2\%}$/ $D_{98\%}$), high dose conformity through prescription isodose to target volume (PITV = 100% Rx isodose volume/PTV_{opt} volume), low dose conformity (D_{2cm} = Maximum dose at 2 cm from PTV_{opt}/Rx dose), and gradient index ($R_{50\%}$ =50% Rx isodose volume/PTV_{opt} volume) for the baseline and adaptive plans. Coverage metrics included target coverage (TC = PTV_{opt} $V_{100\%}$/PTV_{opt} volume) and $D_{90\%}$ and $D_{80\%}$ for GTV, PTV, and PTV_{opt} were also evaluated.

A planning metric for pancreas SBRT that combines indices of GI OAR sparing, PTV/GTV coverage, and conformality into a novel, single global score was developed. Specially, the global plan quality score, or Pancreas Adaptive Radiotherapy Score (*PARTS*) was quantified for adaptive plans and baseline plans. The *PARTS* (**Equation (1)** was quantified as:

$$PARTS = Pancreas\ Adaptive\ Radiotherapy\ Score = M_{GI-OAR} + M_{PTV} + M_{GTV} + \frac{1}{3}M_{D2cm} \quad (1)$$

PARTS combines the following indices: Gastrointestinal Organs at Risk Metric ($M_{GI\text{-}OAR}$, **Equation (2)**, PTV Coverage Metric (M_{PTV}, **Equation (3)**, GTV Coverage Metric (M_{GTV}, **Equation (4)**, and Conformality Metric of D_{2cm} (M_{D2cm}, **Equation (5)**:

$$M_{GI-OAR} = Gastrointestinal\ Organs\ at\ Risk\ Metric = 1 - \sum_{n=1}^{\#GIOARs} \frac{\left(\frac{1}{2} * \frac{V_{x[Gy]}}{0.03} + \frac{1}{2} * \frac{V_{y[Gy]}}{0.5}\right)}{n} \quad (2)$$

where x denotes 40 Gy and y denotes 35 Gy for stomach, duodenum, and small bowel; for large bowel, x denotes 43 Gy and y denotes 38 Gy.

$$M_{PTV} = PTV\ Coverage\ Metric = \sqrt{\frac{1}{3} * \frac{D_{90\%}}{50} + \frac{1}{3} * \frac{D_{80\%}}{50} + \frac{1}{3} * \left(\frac{D_{mean}}{50}\right)^2} \quad (3)$$

$$M_{GTV} = GTV\ Coverage\ Metric = \sqrt{\frac{1}{3} * \frac{D_{90\%}}{50} + \frac{1}{3} * \frac{D_{80\%}}{50} + \frac{1}{3} * \left(\frac{D_{mean}}{50}\right)^2} \quad (4)$$

$$M_{D2cm} = Conformality\ Metric\ of\ D_{2cm} = \frac{D_{2cm-RTOG[\%]}}{D_{2cm[\%]}} \quad (5)$$

Note that **Equation (5)** is normalized to the D_{2cm} metric from RTOG 0813, and is $D_{2cm\text{-}RTOG[\%]}$. For implementation of $D_{2cm\text{-}RTOG[\%]}$, we interpolated the ideal maximum dose, normalized to the plan's prescription, at 2 cm from the PTV, per the RTOG 0813 protocol, based on the volume of the PTV used in the treatment plan being assessed.

Results

The plan quality metrics for conformality, coverage, and degree of modulation across the 67 patients are displayed for the baseline plans (n = 67) and adaptive plans (n = 318) in Table 1. Mean ± SD coverage for baseline plans and across all adaptive plans were 47.4 ± 4.7 Gy and 46.6 ± 6.1 Gy (PTV_{opt} $D_{90\%}$), 50.1 ± 4.2 Gy and 49.1 ± 4.7 Gy (PTV_{opt} $D_{80\%}$), and 80% ± 18% and 74% ± 18% (TC), respectively. Mean ± SD homogeneity and conformity indices for baseline and adaptive plans were 0.87 ± 0.25 and 0.81 ± 0.30 (PITV), 3.81 ± 1.87 and 3.87 ± 2.0 ($R_{50\%}$), 1.53 ± 0.23 and 1.55 ± 0.23 (HI), and 58% ± 7% and 59% ± 7% (D_{2cm}), respectively. Mean ± SD *PARTS* for baseline and adaptive plans were 3.30 ± 0.19 and 3.10 ± 0.23, respectively. For all treatment plans, the total number of beams mean ± SD was 15.8 ± 1.9 (range: 12–21) and total number of segments was 46.4 ± 9.2 (range: 25–91). OAR constraints were met on all baseline and adaptive plans.

Adaptive robustness (baseline plan to fraction 1) and adaptive stability (fractions with the smallest to largest variance in overlapping GI organs as quantified through PTV_{opt}/PTV) was quantified for statistical difference and is listed in Table 1, along with the median value for the respective metric. No statistically significant differences were found for plan quality for adaptive stability, except for *PARTS* ($p = 0.04$, median difference −0.6%). For adaptive robustness statistical differences when significant were small for most metrics (i.e., <2% median differences), with exception of 5% median loss of TC, PITV, and *PARTS*.

Statistical comparison was performed on baseline plans to quantify the difference in planning technique of the PRV_{GI} margin (3 mm versus 5 mm) and number of beams (12–15 beams versus 16–21 beams). To this end, a Kolmogorov-Smirnov test was used to compare of non-normal distributions of unequal size (i.e., 29 versus 38 patients for PRV_{GI} margin; 32 versus 35 patients for beam arrangement). The distribution of the indices was the same across both the groups of PRV_{GI} margin and beam arrangement ($p > 0.05$).

Downloaded for Anonymous User (n/a) at Baptist Health South Florida Inc from ClinicalKey.com by Elsevier on May 10, 2024. For personal use only. No other uses without permission. Copyright ©2024. Elsevier Inc. All rights reserved.

Table 1
Plan quality and modulation metrics between baseline plans (n = 67 plans) and adaptive plans (n = 318 plans) for dose conformality, target coverage, and beam parameters for 67 patients with adaptive robustness (baseline plan to fraction 1) and adaptive stability (fractions with minimum and maximum PTV_{opt}/PTV) quantified for statistical difference. Note: Pancreas Adaptive Radiotherapy Score (*PARTS*), Gastrointestinal Organs at Risk Metric (M_{GI-OAR}), PTV coverage Metric (M_{PTV}), GTV coverage Metric (M_{GTV}), Conformality metric of D_{2cm} (M_{D2cm}).

Metric		Metric Unit	Baseline plans			Online adaptive plans			Online adaptive robustness		Online adaptive stability	
			median	mean	SD	median	mean	SD	p-value (baseline to fx 1)	% difference in median (baseline to fx 1)	p-value (min to max fx)	% difference in median (min to max fx)
Conformality	PITV	Ratio of Rx iso vol to PTV_{opt} vol	0.87	0.87	0.25	0.80	0.81	0.30	p < 0.01	−5.0%	p = 0.41	−3.8%
	$R_{50\%}$	Ratio of 50% Rx iso vol to PTV_{opt} vol	3.36	3.81	1.87	3.36	3.87	2.00	p = 0.12	−0.6%	p = 0.38	−1.1%
	HI	PTV_{opt} $D_{2\%}$/PTV_{opt} $D_{98\%}$	1.52	1.53	0.23	1.54	1.55	0.23	p < 0.01	2.9%	p = 0.31	1.8%
	D_{2cm}	[in % of prescribed dose] at 2 cm from PTV_{opt} in any direction	0.57	0.58	0.07	0.58	0.59	0.07	p = 0.17	2.3%	p = 0.47	−2.7%
Target coverage	Volume PTV_{opt}	[cc]	76.84	82.02	41.77	105.06	109.47	62.49				
	TC	Ratio PTV_{opt} vol receiving Rx dose to PTV_{opt} vol	0.84	0.80	0.18	0.77	0.74	0.18	p < 0.01	−5.4%	p = 0.36	−4.6%
	PTV_{opt} D90%	[Gy]	48.03	47.39	4.69	46.70	46.58	6.06	p < 0.01	−2.3%	p = 0.48	−1.5%
	PTV_{opt} D80%	[Gy]	50.74	50.06	4.22	49.42	49.08	4.73	p < 0.01	−1.7%	p = 0.34	−1.5%
	PTV D90%	[Gy]	39.26	40.47	6.40	39.58	39.87	6.13	p = 0.03	−0.7%	p = 0.9	0.7%
	PTV D80%	[Gy]	44.73	44.88	5.82	45.05	44.27	5.50	p < 0.01	−1.7%	p = 0.93	0.6%
	PTV mean	[Gy]	52.62	51.83	3.99	51.72	50.99	3.92	p < 0.01	−1.7%	p = 0.28	−1.0%
	PTV max	[Gy]	68.64	67.92	4.04	68.40	67.75	5.04	p = 0.53	−0.2%	p = 0.25	−1.3%
	GTV D90%	[Gy]	49.29	48.48	6.14	47.89	47.63	6.59	p = 0.22	−2.4%	p = 0.83	−2.0%
	GTV $D_{80\%}$	[Gy]	52.95	52.36	4.98	51.54	51.21	5.23	p = 0.03	−1.7%	p = 0.77	−1.3%
	GTV mean	[Gy]	57.27	56.74	3.77	56.22	55.91	4.04	p = 0.08	−1.3%	p = 0.58	−0.3%
	GTV max	[Gy]	68.33	67.66	4.15	68.31	67.63	4.95	p = 0.55	−0.2%	p = 0.33	−0.6%
Modulation	Beams	number of total beams	16.00	15.89	1.88	16.00	15.85	1.89	p = 1	0.0%	p = 0.31	0.0%
	Segments	number of total segments	45.00	46.17	8.71	45.00	46.20	9.43	p = 0.22	0.0%	p = 0.05	0.0%
PARTS	Plan quality	$M_{GI-OAR} + M_{PTV} + M_{GTV} + \frac{1}{3}M_{D2cm}$	3.32	3.30	0.19	3.11	3.10	0.23	p < 0.01	−5.7%	p = 0.04	−0.6%

Fig. 3 displays the boxplot of coverage to the GTV and PTV metrics including mean, maximum, $D_{90\%}$, and $D_{80\%}$ for adaptive stability of the fractions with the minimum and maximum PTV_{opt}/PTV (Fig. 3**A**), adaptive robustness of baseline plan to fraction 1 (Fig. 3**B**), and for baseline plans to all adaptive plans (Fig. 3**C**). The boxplot displays the median, 1st quartile, 3rd quartile, and range. The whiskers represent 1.5 times the interquartile range with data outside this range displayed as outliers. Fig. 3**C** depicted more outliers for the adaptive plans and hence we performed Welch test between the baseline and adaptive plans, which was not statistically significantly different indicating no unequal variance between the groups.

Fig. 4 displays the boxplot conformality and adaptive plan score metrics including HI, PITV, D_{2cm}, $R_{50\%}$, and *PARTS* for adaptive stability of the fractions with the minimum and maximum PTV_{opt}/PTV (Fig. 4**A**), adaptive robustness of baseline plan to fraction 1 (Fig. 4**B**), and for baseline plans to all adaptive plans (Fig. 4**C**). The boxplot displays the median, 1st quartile, and 3rd quartile, with whiskers representing 1.5 times the interquartile range, and outliers not displayed due to axis range. Similar medians and ranges are observed in conformality and *PARTS* metrics between baseline and adaptive plans.

The adaptive doses versus predicted doses of the GI OARs for all delivered fractions are shown in Fig. 5. Since the adaptive plans were normalized based on an isotoxicity model to neighboring GI OARs, all OARs were at or under prescribed constraint of $D_{0.5cc}$. For the predicted doses, large differences in GI OAR anatomy within the high dose gradient on the anatomy of the day demonstrate violations of the $D_{0.5cc}$ GI luminal OAR constraint, and hence validating the indication for adaptation. The mean ± SD $V_{35\ Gy}$ for stomach, duodenum, and small bowel was 1.4 ± 2.6 cc and 0.1 ± 0.2 cc for the predicted and adaptive doses, respectively. Most predicted dose variability was observed for the duodenum $V_{35\ Gy}$ (Fig. 5). The mean ± SD $V_{38\ Gy}$ for large bowel was more similar at 0.1 ± 0.3 cc and 0.0 ± 0.1 cc for the predicted and adaptive doses, respectively.

Discussion

To our knowledge, this is the first report of a planning technique for 50 Gy in 5 fraction SMART using a treatment planning platform in its existing state (i.e., no neural network). We evaluated the robustness and stability of online adaptive plan quality using this planning technique for the treatment of inoperable PCa patients prescribed 50 Gy in 5 fractions (BED_{10} = 100 Gy_{10}) including a typically generous hotspot exceeding 60–70 Gy (BED_{10} > 130–160 Gy). This extreme dose escalation has historically not been safely achievable using x-ray or CT guidance [19] due to large, interfractional spatial changes of GI OARs with respect to the target—

Downloaded for Anonymous User (n/a) at Baptist Health South Florida Inc from ClinicalKey.com by Elsevier on May 10, 2024. For personal use only. No other uses without permission. Copyright ©2024. Elsevier Inc. All rights reserved.

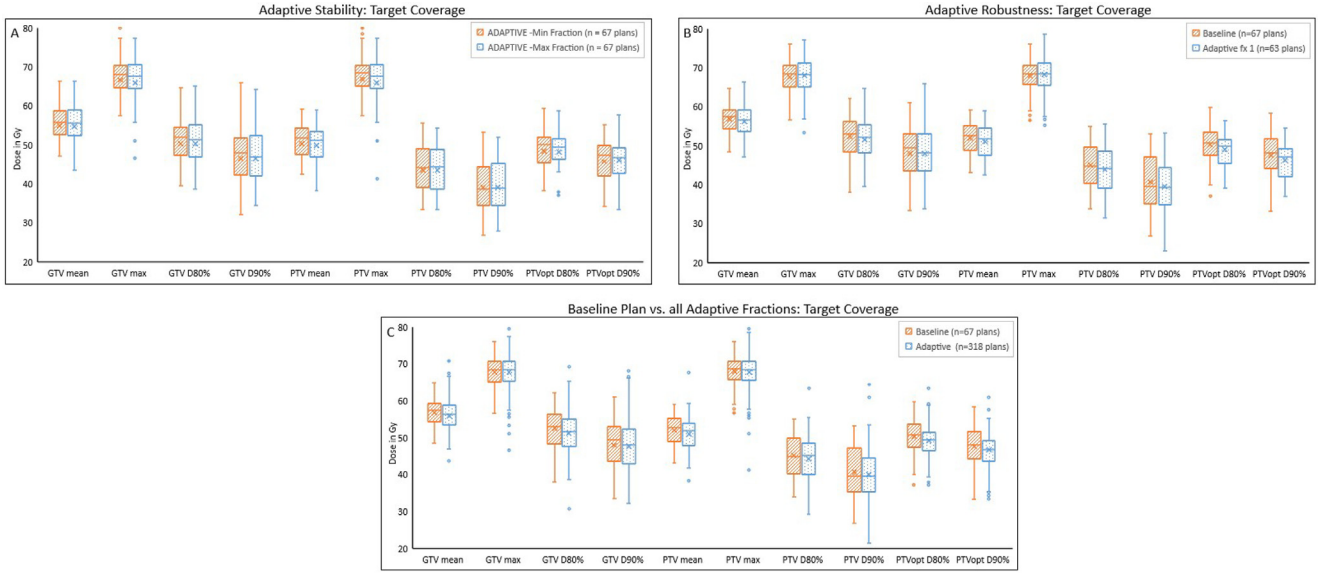

Fig. 3. Boxplot of target coverage for gross tumor volume (GTV) and planning target volume (PTV) metrics including mean, maximum, $D_{90\%}$ and $D_{80\%}$ for adaptive stability of fractions with minimum and maximum PTV_{opt}/PTV (**A**), adaptive robustness of baseline plan to fraction 1 (**B**), and for baseline plans to all adaptive plans (**C**).

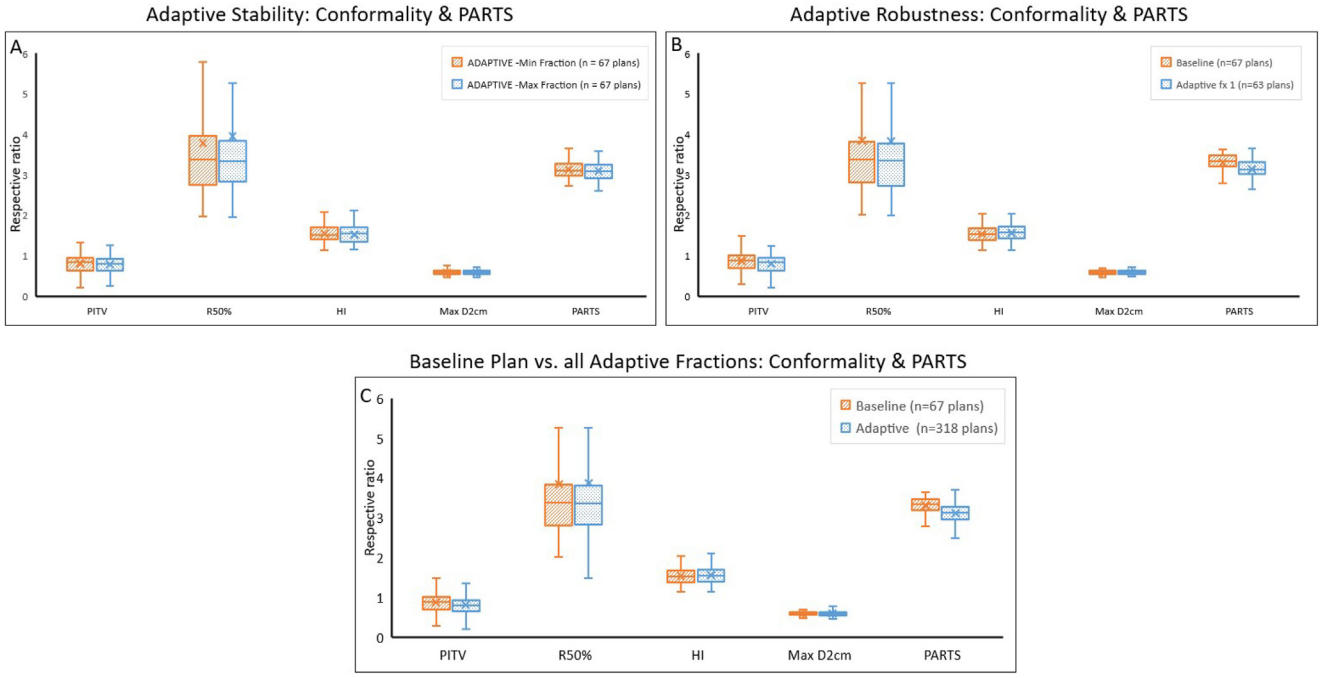

Fig. 4. Boxplot conformality metrics including homogeneity index (HI), prescription isodose to target volume (PITV), low dose conformity (D_{2cm}), gradient ($R_{50\%}$), and Pancreas Adaptive Radiotherapy Score (*PARTS*) for adaptive stability of fractions with minimum and maximum PTV_{opt}/PTV (**A**), adaptive robustness of baseline plan to fraction 1 (**B**), and for baseline plans to all adaptive plans (**C**).

although a recently reported phase 2 trial of 50 Gy in 5 fractions demonstrated that ablative dose can be safely delivered using on-table adaptive replanning on a 0.35 T MR-guided system [20].

In this work, we coin the term "robustness" in the context of on-table adaptive radiotherapy to refer to the interfractional plan quality of the on-table adaptive plan derived from the optimization objectives set created from the initial simulation plan. Current practice is to employ a manual-based cost function edits to a set of optimization objectives during on-table adaptive re-planning to result in a plan with a robust solution to the anatomy of the day. Future development in adaptive radiotherapy could deploy automatic adjustment to the cost function based on the interfractional geometry changes on the anatomy of the day using AI-based approaches. Specially, Nguyen *et al.* demonstrated the ability to predict dose distribution with input of geometry for prostate plans using a convolutional deep network model. As such, predicting the optimal dose could be advantageous for adaptive radiotherapy. This approach would potentially reduce planning time and uncertainty of the global solution by providing planner with the known optimal dose distribution [21].

For intrafractional anatomical changes (i.e., GI peristalsis), robust optimization could be deployed in future adaptive RT devel-

Downloaded for Anonymous User (n/a) at Baptist Health South Florida Inc from ClinicalKey.com by Elsevier on May 10, 2024. For personal use only. No other uses without permission. Copyright ©2024. Elsevier Inc. All rights reserved.

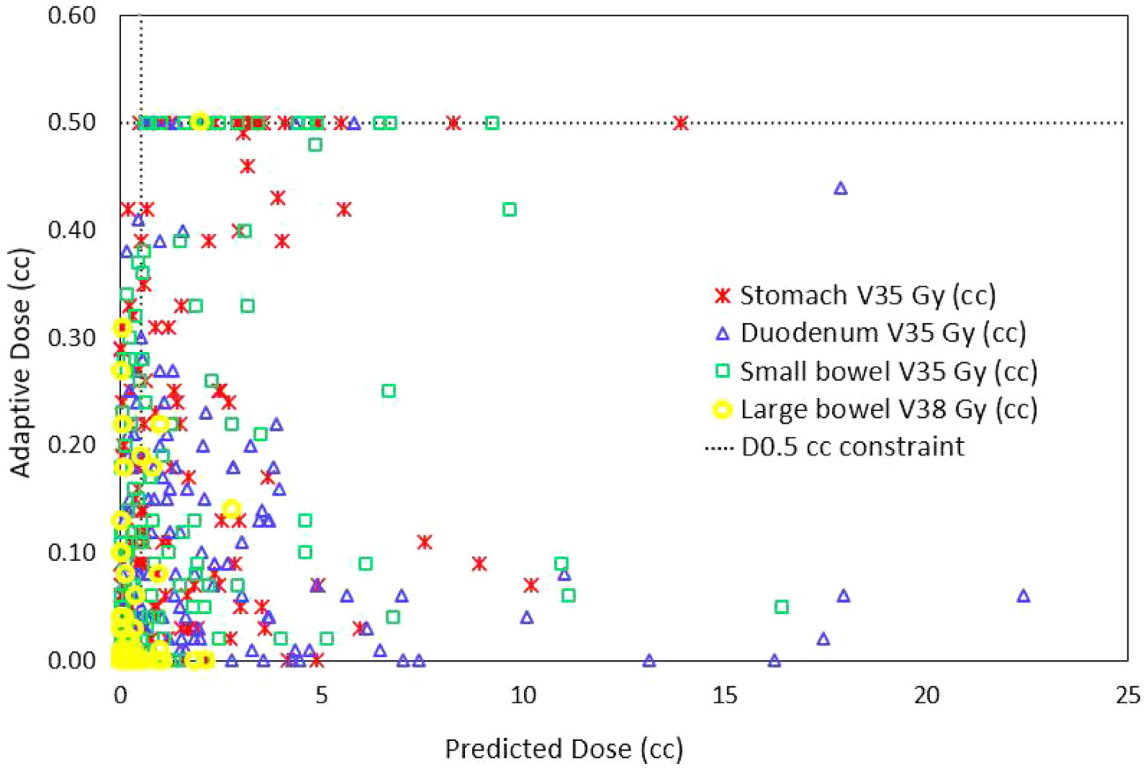

Fig. 5. Plan quality differences to the GI luminal OARs between adaptive doses and predicted doses (i.e., initial plan recalculated on fractional MR anatomy of day) for the volumes receiving 35 Gy ($V_{35\ Gy}$) to the stomach, duodenum, and small bowel and the volume receiving 38 Gy ($V_{38\ Gy}$) to large bowel.

opment. As such, these intrafractional anatomical changes are random in nature therefore incorporating a predictive motion map for random changes would be challenging in terms of using a robust optimization-margin approach. Enabling mid-treatment adaptation when GI peristalsis exceeds a known limit of margin could be a potential solution for deployment of robust intrafraction optimization, if imaging capabilities enable acquisition of peristalsis throughout the treatment delivery.

Chow *et al.* and van Timmeren *et al.* retrospectively evaluated the plan quality for PCa adaptive RT using 33–40 Gy in 5 fractions in a series of 74 and 15 adaptive fractions, respectively [12,13]. With an ablative dose of 50 Gy in 5 fractions increasingly being delivered using SMART, there is a significant clinical need to understand the achievable plan quality from on-table adaptation. Moreover, the isotoxicity approach to maintain GI OAR constraints while intentionally under-covering target coverage goals makes this anatomical site unique and makes the comparison to previously published plan quality studies on other disease sites inapplicable. Therefore, this work is central in benchmarking pancreas SBRT plan quality at ablative doses in the online adaptive setting. Our planning approach is correlated to the clinical outcomes and toxicities of our first thirty pancreatic patients included in this study as recently reported in our companion work, within which SMART was found safe with minimal (<3%) grade 3 toxicities using this planning approach and excellent 1-year local control at 88% [10].

Our adaptive planning approach defined the location of the 30 Gy, 50 Gy, and 60 Gy dose gradients and dynamically-updated the gradient position based on the anatomical position of the GI OAR of the day through predefined Boolean operations and margin expansions/contractions. The ablative dose region (i.e., >50 Gy) was safely positioned away from the GI OAR by creation of the GTV_{core}, reducing the likelihood of unintended GI overdosing during routine intrafractional GI peristalsis throughout the adaptive planning process and treatment delivery. Adaptive RT is particularly beneficial for treating anatomical sites in which interfraction motion causes changes in position of proximal OAR to target [7,13,22,23]. As such, this planning approach extends beyond pancreatic SMART and has been deployed for all anatomical sites for SMART at our institution for which sizeable interfractional OAR-to-target geometry changes are anticipated.

Our adaptive planning approach utilizes two sets of conformality rings: $Ring_{2cm}$ and $Ring_{LowDose}$. Conformality was emphasized in our planning technique for two reasons: (1) to reduce impact of GI peristalsis (2) to limit partial segmentation of OARs during adaptive segmentation to only the high dose region. Our online ablative segmentation approach segments any OAR overlapped within 2 cm cranial-caudal and 3 cm axially to PTV_{opt} surface. Therefore, confining conformality of the 50–60% isodose lines to within the $Ring_{2cm}$ eliminates OAR violation from any unsegmented regions that would not show up in adaptive plan statistics or DVH parameter. Additionally, SBRT metrics of D_{2cm} are easily visualized during adaptive replanning through visual inspection of relevant isodose lines and $Ring_{2cm}$.

Our planning technique was evaluated using the *PARTS*, which is based on four aspects of SBRT pancreas planning: GI luminal OAR doses, PTV coverage, GTV coverage, and conformality. Each metric of the *PARTS* was designed to approach 1.0, individually, in an ideal setting. However, an individual metric may slightly exceed 1.0 if the coverage to the targets exceeded the prescription, which is likely to occur in the GTV Coverage Metric. Note that the PTV and GTV Coverage Metrics are weighted averages of the three target criteria used to evaluate coverage: $D_{80\%}$, $D_{90\%}$, and mean dose. The purpose of the square root was to bring values greater than 1.0 back to 1.0, and mean dose to the targets was squared such that any under coverage would be greater penalized. The Conformality Metric of D_{2cm} takes into account the size of the PTV, when evaluating the intermediate dose falloff and is normalized based on the RTOG 0813 conformality goals. The Gastrointestinal

Downloaded for Anonymous User (n/a) at Baptist Health South Florida Inc from ClinicalKey.com by Elsevier on May 10, 2024. For personal use only. No other uses without permission. Copyright ©2024. Elsevier Inc. All rights reserved.

Organs at Risk Metric was normalized to the 0.03 cc and 0.5 cc volumes as a weighted average of all GI OARs which measures isotoxicity. We believe our planning score (i.e., *PARTS*) to be both flexible and sensitive. Specifically, we found that the *PARTS* had greater sensitivity than the individual metrics that it comprised of. For example, adaptive robustness (Table 1) had a median *PARTS* of 5.7% which was greater than the individual plan quality metrics.

PARTS was found to be more sensitive than the individual metrics incorporated into **Equation (1)**. For example, while no individual metric showed statistical significance for adaptive stability, *PARTS* demonstrated a statistical difference (p = 0.04), although median difference was only 0.6%. Similarly for adaptive robustness, the greatest median percentage difference was seen for *PARTS* at 5.7% (Table 1). We believe this phenomenon is related to the impact of interfractional OAR-PTV geometry change on each of the *PARTS*' sub-metrics. For example, a "favorable" geometry during adaptation would potentially allow an isocoverage approach, in which the full prescription was achieved to the targets with OARs below constraints. On the other hand, an "unfavorable" geometry during adaptation would require the typical isotoxicity approach, necessitating undercoverage of the targets and and/or reduction in conformality to achieve OAR constraints. The additive relationship of **Equation (1)** would amplify the cost of "unfavorable" geometry and conversely amplify the reward of "favorable" geometry.

This work is the first reporting of an adaptive plan quality metric in the literature. Currently, plan quality metrics are limited to include only metric of conformality and/or coverage such as Akapti *et al.* for radiosurgery cases [24]. Other approaches are limited to only PTV and OAR indices, such as Journet *et al.* [25]. While Nelms *et al.* approach utilized coverage, OAR, and conformality goals [26], the OAR metrics related to the percentage of the ROI receiving a dose—an impractical solution for adaptive RT, in which only partial segmentation of the OAR in the high dose regions is performed. A modified approach of these plan quality scores could be implemented to make consistent with the practice of adaptive pancreas RT, in which maximum GI OAR doses, intermediate dose conformality, and target coverage drive the adaptive plan quality.

Adaptive plans were equivalent to baseline plans. There were no statistical differences between adaptive fractions (i.e., stability), except for *PARTS*. And statistical differences between baseline and adaptive plan quality metrics (i.e., robustness) when significant were small for most metrics (<2.0% median differences) with exception of 5% median loss of TC, PITV, and *PARTS*. GI OAR constraints were met for all adaptive plans due to our isotoxicity planning approach (Fig. 5). Since the planning technique was robust to GI interfractional anatomical changes between simulation and daily adaptive treatment, this study's findings point towards the potential utility of a patient-agnostic planning approach to create the baseline plan [27,28], owing to the planning strategy of updating dosimetric gradients in real-time by pre-defined Boolean operations.

A key strength of this strategy is its elegant simplicity. Fewer rules reduce the potential for error propagation throughout the process, and this is advantageous for workflow. Bohoudi *et al.* described an approach of using an ANN model in the adaptive treatment of 40 Gy in 5 fractions to the pancreas [11,29]. Their OAR partial segmentation included dividing the OAR into 1 cm, 2 cm, and 3 cm distances from the PTV. Our approach does not subdivide the OAR. We simply manually edited from the deformed OAR that was proximal within 3 cm of the target. Therefore, our optimization objectives and planning criteria is simplified by having fewer subdivided segmentation, which may reduce error propagation via mitigation of greater segmentational complexity. Our technique does not require an ANN, in turn making it more accessible. Another distinction is that our ablative dose was driven hotter, the $D_{1\%}$ was up to 125% of the prescribed dose of 40 Gy for the plan quality described by Bohoudi *et al*, and our $D_{2\%}$ was up to 155% of the prescribed dose of 50 Gy [11,29].

Olberg *et al.* defined a more simplistic approach in combining the GI OARs into a unified ROI for a non-SBRT course to the pancreas [30]. Rather than a unified GI OAR proposed by Olberg *et al.*, our approach similar to Bohoudi *et al.* found utility of controlling the dosimetric gradient through respective optimization objectives based on position of OAR with respect to target. Our technique of having a different objective available potentially enabled higher plan quality for baseline and at time of on-table adaptation. For example, our method allowed "hitting" the relevant OAR (i.e., duodenum) that was dosimetrically exceeding on the anatomy of the day due to larger degree of overlap into the PTV, without penalizing another GI OAR far away from the target well within tolerance (i.e., large bowel), thereby simplifying the overall change to the cost function from initial planning.

Additional studies have proposed adaptive planning strategies to reduce on-table time and frequency. Van Timmeren *et al.* compared segment-weight re-optimization to a full IMRT re-optimization and found for anatomical sites where the OAR was close or within the PTV that a full IMRT re-optimization was required due to large anatomical changes, such as observed in pancreas cancer [31]. Böck *et al.* proposed an online adaptive RT framework using Bayesian inference which may improve optimization robustness based on geometrical interfractional variations and reduce adaptation frequency [32]. Liu *et al.* proposed integration of the intensity field projection algorithm to adjust intensity of each beam based on the deformation of structures. Specifically by converting 3D deformation vectors into 2D deformation field corresponding to the beam orientation and then generate a new corresponding beam intensity was able to decrease overall optimization time to 3 minutes [33].

One limitation of our approach is that it potentially requires multiple iterations for on-table adaptive re-optimization compared to the approach by Bohoudi *et al.* [11,29]. Although there was greater potential for more iterations, our online adaptive re-planning technique was still clinically acceptable with a median of two re-optimization iterations.

In conclusion, we demonstrate that 5-fraction SMART prescribed to an ablative dose for inoperable pancreatic cancer can be routinely delivered with similar robustness and stability. High plan quality was maintained on the adaptive plans from the inherent robustness of using a GI PRV-driven planning technique despite substantial GI interfraction motion causing daily changes in the spatial position of the dosimetric gradient. Planning rings enabled robustness in dose conformity. This work supports the feasibility towards utilizing a patient-independent, template baseline plan as a starting point for daily on-table adaptive plans to reduce the upfront planning time and resource utilization.

Conflict of interest

Dr. Chuong reports personal fees from ViewRay Inc, personal fees from Sirtex, personal fees from Advanced Accelerator Applications, grants from ViewRay Inc, grants from AstraZeneca, grants from Novocure, outside the submitted work.

Dr. Kotecha reports honoraria from Accuray Inc., Elekta AB, ViewRay Inc., Novocure Inc., Elsevier Inc., Brainlab, Kazia Therapeutics, Castle Biosciences, and institutional research funding from Medtronic Inc., Blue Earth Diagnostics Ltd., Novocure Inc., GT Medical Technologies, AstraZeneca, Exelixis, ViewRay Inc., Brainlab, Cantex Pharmaceuticals, and Kazia Therapeutics.

Dr Mehta: Honoraria: Zap, Mevion, Karyopharm, Tocagen, Astra Zeneca; BOD: Oncoceutics.

Downloaded for Anonymous User (n/a) at Baptist Health South Florida Inc from ClinicalKey.com by Elsevier on May 10, 2024. For personal use only. No other uses without permission. Copyright ©2024. Elsevier Inc. All rights reserved.

Dr. Gutierrez: Honoraria: Elekta, ViewRay, Inc.

Dr. Bassiri reports grants from ViewRay Inc, outside the submitted work.

Dr. Mittauer reports personal fees from ViewRay Inc, other from MR Guidance LLC, grants from ViewRay Inc, outside the submitted work.

CRediT authorship contribution statement

Kathryn E Mittauer: Conceptualization, Methodology, Investigation, Formal analysis, Writing – original draft, Writing – review & editing. **Sreenija Yarlagadda:** Investigation, Formal analysis, Writing – review & editing. **John M. Bryant:** Investigation, Writing – original draft. **Nema Bassiri:** Formal analysis, Methodology, Writing – review & editing. **Tino Romaguera:** Methodology. **Andres G Gomez:** Investigation. **Robert Herrera:** Investigation. **Rupesh Kotecha:** Writing – review & editing. **Minesh P Mehta:** Writing – review & editing. **Alonso N Gutierrez:** Formal analysis, Methodology, Writing – review & editing. **Michael D Chuong:** Conceptualization, Methodology, Writing – review & editing.

Declaration of Competing Interest

The authors declare the following financial interests/personal relationships which may be considered as potential competing interests: Kathryn Mittauer reports a relationship with ViewRay Inc that includes: consulting or advisory, funding grants, speaking and lecture fees, and travel reimbursement. Kathryn Mittauer reports a relationship with MR Guidance LLC that includes: equity or stocks. Nema Bassiri reports a relationship with ViewRay Inc that includes: funding grants. Alonso N Gutierrez reports a relationship with ViewRay Inc that includes: speaking and lecture fees. Alonso N Gutierrez reports a relationship with Elekta AB that includes: speaking and lecture fees. Alonso N Gutierrez reports a relationship with IBA that includes: speaking and lecture fees. Alonso N Gutierrez reports a relationship with Uplan that includes: equity or stocks. Minesh P Mehta reports a relationship with Karyopharm that includes: consulting or advisory. Minesh P Mehta reports a relationship with Kazia Therapeutics Limited that includes: consulting or advisory. Minesh P Mehta reports a relationship with Sapience that includes: consulting or advisory. Minesh P Mehta reports a relationship with Zap that includes: consulting or advisory. Minesh P Mehta reports a relationship with Mevion that includes: consulting or advisory. Minesh P Mehta reports a relationship with Xoft that includes: consulting or advisory. Minesh P Mehta reports a relationship with Oncoceutics that includes: board membership. Minesh P Mehta reports a relationship with Chimerix that includes: equity or stocks. Michael D Chuong reports a relationship with ViewRay that includes: consulting or advisory, funding grants, speaking and lecture fees, and travel reimbursement. Michael D Chuong reports a relationship with Sirtex that includes: speaking and lecture fees. Michael D Chuong reports a relationship with IBA that includes: speaking and lecture fees. Michael D Chuong reports a relationship with Novocure that includes: funding grants. Michael D Chuong reports a relationship with StratPharma that includes: funding grants. Dr. Kotecha reports personal fees from Accuray Inc, personal fees from Elekta AB, grants and personal fees from ViewRay Inc, grants and personal fees from Novocure Inc, personal fees from Elsevier Inc, grants and personal fees from Brainlab, grants and personal fees from Kazia Therapeutics, personal fees from Castle Biosciences, grants from Medtronic Inc, grants from Blue Earth Diagnostics Ltd, grants from GT Medical Technologies, grants from AstraZeneca, grants from Exelixis, grants from Cantex Pharmaceuticals, during the conduct of the study.

Appendix A. Supplementary material

Supplementary data to this article can be found online at https://doi.org/10.1016/j.radonc.2023.109869.

References

[1] Yan D, Vicini F, Wong J, Martinez A. Adaptive radiation therapy. Phys Med Biol 1997 Jan;42:123–32. https://doi.org/10.1088/0031-9155/42/1/008. PMID: 9015813.

[2] Sonke JJ, Aznar M, Rasch C. Adaptive radiotherapy for anatomical changes. Semin Radiat Oncol 2019 Jul;29:245–57. https://doi.org/10.1016/j.semradonc.2019.02.007. PMID: 31027642.

[3] Mittauer K, Paliwal B, Hill P, Bayouth JE, Geurts MW, Baschnagel AM, et al. A new era of image guidance with magnetic resonance-guided radiation therapy for abdominal and thoracic malignancies. Cureus 2018 Apr 4;10:e2422. https://doi.org/10.7759/cureus.2422. PMID: 29872602 PMCID: PMC5985918.

[4] Güngör G, Serbez İ, Temur B, Gür G, Kayalılar N, Mustafayev TZ, Korkmaz L, Aydın G, Yapıcı B, Atalar B, Özyar E. Time Analysis of Online Adaptive Magnetic Resonance-Guided Radiation Therapy Workflow According to Anatomical Sites. Pract Radiat Oncol. 2021 Jan-Feb;11:e11-e21. doi: 10.1016/j.prro.2020.07.003. Epub 2020 Jul 30. PMID: 32739438.

[5] Boldrini L, Cusumano D, Cellini F, Azario L, Mattiucci GC, Valentini V. Online adaptive magnetic resonance guided radiotherapy for pancreatic cancer: state of the art, pearls and pitfalls. Radiat Oncol 2019 Apr 29;14:71. https://doi.org/10.1186/s13014-019-1275-3. PMID: 31036034 PMCID: PMC6489212.

[6] El-Bared N, Portelance L, Spieler BO, Kwon D, Padgett KR, Brown KM, et al. Dosimetric benefits and practical pitfalls of daily online adaptive MRI-guided stereotactic radiation therapy for pancreatic cancer. Pract Radiat Oncol 2019 Jan;9:e46–54. https://doi.org/10.1016/j.prro.2018.08.010. Epub 2018 Aug 25 PMID: 30149192.

[7] Henke L, Kashani R, Robinson C, Curcuru A, DeWees T, Bradley J, et al. Phase I trial of stereotactic MR-guided online adaptive radiation therapy (SMART) for the treatment of oligometastatic or unresectable primary malignancies of the abdomen. Radiother Oncol 2018 Mar;126:519–26. https://doi.org/10.1016/j.radonc.2017.11.032. Epub 2017 Dec 23 PMID: 29277446.

[8] Hassanzadeh C, Rudra S, Bommireddy A, Hawkins WG, Wang-Gillam A, Fields RC, et al. Ablative five-fraction stereotactic body radiation therapy for inoperable pancreatic cancer using online MR-guided adaptation. Adv Radiat Oncol 2020 Jun 25;6:. https://doi.org/10.1016/j.adro.2020.06.010. PMID: 33665480 PMCID: PMC7897757100506.

[9] Rudra S et al. Using adaptive magnetic resonance image-guided radiation therapy for treatment of inoperable pancreatic cancer. Cancer Medicine 2019;8:2123–32. https://doi.org/10.1002/cam4.2100.

[10] Chuong MD, Bryant J, Mittauer KE, Hall M, Kotecha R, Alvarez D, Romaguera T, Rubens M, Adamson S, Godley A, Mishra V, Luciani G, Gutierrez AN. Ablative 5-Fraction Stereotactic Magnetic Resonance-Guided Radiation Therapy With On-Table Adaptive Replanning and Elective Nodal Irradiation for Inoperable Pancreas Cancer. Pract Radiat Oncol. 2021 Mar-Apr;11:134-147. doi: 10.1016/j.prro.2020.09.005. Epub 2020 Sep 16.

[11] Bohoudi O, Bruynzeel AME, Senan S, Cuijpers JP, Slotman BJ, Lagerwaard FJ, et al. Fast and robust online adaptive planning in stereotactic MR-guided adaptive radiation therapy (SMART) for pancreatic cancer. Radiother Oncol 2017 Dec;125:439–44. https://doi.org/10.1016/j.radonc.2017.07.028. Epub 2017 Aug 12 PMID: 28811038.

[12] Phillip E. Chow, Fang-I Chu, Nzhde Agazaryan, Minsong Cao, Margeurite Tyran, Yingli Yang, Daniel Low, Ann Raldow, Percy Lee, Michael Steinberg, James M. Lamb, Dosimetric quality of online adapted pancreatic cancer treatment plans on an MRI-guided radiotherapy system, Advances in Radiation Oncology, 2021, 100682, ISSN 2452-1094, https://doi.org/10.1016/j.adro.2021.100682.

[13] van Timmeren JE, Chamberlain M, Krayenbuehl J, Wilke L, Ehrbar S, Bogowicz M, et al. Treatment plan quality during online adaptive re-planning. Radiat Oncol 2020 Aug 21;15:203. https://doi.org/10.1186/s13014-020-01641-0. PMID: 32825848 PMCID: PMC7441614.

[14] Hernandez V, Hansen CR, Widesott L, Bäck A, Canters R, Fusella M, et al. What is plan quality in radiotherapy? The importance of evaluating dose metrics, complexity, and robustness of treatment plans. Radiother Oncol 2020 Dec;153:26–33. https://doi.org/10.1016/j.radonc.2020.09.038. Epub 2020 Sep 25 PMID: 32987045.

[15] Ginn JS, Agazaryan N, Cao M, Baharom U, Low DA, Yang Y, et al. Characterization of spatial distortion in a 0.35 T MRI-guided radiotherapy system. Phys Med Biol 2017 Jun 7;62:4525–40. https://doi.org/10.1088/1361-6560/aa6e1a. Epub 2017 Apr 20 PMID: 28425431 PMCID: PMC6061953.

[16] Placidi L, Nardini M, Cusumano D, Boldrini L, Chiloiro G, Romano A, et al. VMAT-like plans for magnetic resonance guided radiotherapy: Addressing unmet needs. Phys Med 2021 May;85:72–8.

[17] Mittauer KE, Hill PM, Bassetti MF, Bayouth JE. Validation of an MR-guided online adaptive radiotherapy (MRgoART) program: Deformation accuracy in a heterogeneous, deformable, anthropomorphic phantom. Radiother Oncol 2020 May;146:97–109. https://doi.org/10.1016/j.radonc.2020.02.012. Epub 2020 Mar 6 PMID: 32146260.

[18] Rodriguez LL, Kotecha R, Tom MC, Chuong MD, Contreras JA, Romaguera T, et al. CT-guided versus MR-guided radiotherapy: Impact on gastrointestinal sparing in adrenal stereotactic body radiotherapy. Radiother Oncol 2022

Downloaded for Anonymous User (n/a) at Baptist Health South Florida Inc from ClinicalKey.com by Elsevier on May 10, 2024. For personal use only. No other uses without permission. Copyright ©2024. Elsevier Inc. All rights reserved.

Jan;166:101–9. https://doi.org/10.1016/j.radonc.2021.11.024. Epub 2021 Nov 26 PMID: 34843842.
[19] Colbert LE, Rebueno N, Moningi S, Beddar S, Sawakuchi GO, Herman JM, et al. Dose escalation for locally advanced pancreatic cancer: How high can we go? Adv Radiat Oncol 2018 Oct 23;3:693–700. https://doi.org/10.1016/j.adro.2018.07.008. PMID: 30370371 PMCID: PMC6200902.
[20] Parikh PJ, Lee P, Low DA, Kim J, Mittauer KE, Bassetti MF, Glide-Hurst CK, Raldow AC, Yang Y, Portelance L, Padgett KR, Zaki B, Zhang R, Kim H, Henke LE, Price AT, Mancias JD, Williams CL, Ng J, Pennell R, Pfeffer MR, Levin D, Mueller AC, Mooney KE, Kelly P, Shah AP, Boldrini L, Placidi L, Fuss M, Chuong MD. A Multi-Institutional Phase 2 Trial of Ablative 5-Fraction Stereotactic Magnetic Resonance-Guided On-Table Adaptive Radiation Therapy for Borderline Resectable and Locally Advanced Pancreatic Cancer. Int J Radiat Oncol Biol Phys. 2023 May 19:S0360-3016 00499-6. doi: 10.1016/j.ijrobp.2023.05.023. Epub ahead of print. PMID: 37210048.
[21] Nguyen D, Long T, Jia X, et al. A feasibility study for predicting optimal radiation therapy dose distributions of prostate cancer patients from patient anatomy using deep learning. Sci Rep 2019;9:1076. https://doi.org/10.1038/s41598-018-37741-x.
[22] Jacob S Witt MD, Stephen A Rosenberg MD and Michael F Bassetti MRI-guided adaptive radiotherapy for liver tumours: visualising the future Lancet Oncology, The, 2020-02-01, Volume 21, Pages e74-e82.
[23] Tetar SU, Bruynzeel A, Lagerwaard FJ, Slotman BJ, Bohoudi O, Palacios MA. Clinical implementation of magnetic resonance imaging guided adaptive radiotherapy for localized prostate cancer. Phys Imaging Radiat Oncol 2019;9:69–76.
[24] Akpati H et al. Unified dosimetry index (UDI): a figure of merit for ranking treatment plans. JACMP 2008 Jun 23;9:99–108.
[25] Jornet N et al. Multicentre validation of IMRT pre-treatment verification: comparison of in-house and external audit. Radiother Oncol 2014. Sep;112:381–8.
[26] Nelms BE et al. Variation in external beam treatment plan quality: An inter-institutional study of planners and planning systems. Pract Radiat Oncol. 2012 Oct-Dec;2:296-305.
[27] Cilla S, Ianiro A, Romano C, et al. Template-based automation of treatment planning in advanced radiotherapy: a comprehensive dosimetric and clinical evaluation. Sci Rep 2020;10:423. https://doi.org/10.1038/s41598-019-56966-y.
[28] K.E. Mittauer, R. Herrera, M.D. Chuong, J. Contreras, D. Alvarez, T. Romaguera, R. Kotecha, M.D. Hall, M.P. Mehta, A. Gutierrez A Novel Pre-plan Technique for On-table Adaptation of Pancreatic Stereotactic MR-guided Online Adaptive Radiotherapy V108, IJROBP, S187-S188, 2020.
[29] Bohoudi O, Bruynzeel AME, Meijerink MR, Senan S, Slotman BJ, Palacios MA, et al. Identification of patients with locally advanced pancreatic cancer benefitting from plan adaptation in MR-guided radiation therapy. Radiother Oncol 2019 Mar;132:16–22. https://doi.org/10.1016/j.radonc.2018.11.019. Epub 2018 Dec 20 PMID: 30825964.
[30] Olberg S, Green O, Cai B, et al. Optimization of treatment planning workflow and tumor coverage during daily adaptive magnetic resonance image guided radiation therapy (MR-IGRT) of pancreatic cancer. Radiat Oncol 2018;13:51. https://doi.org/10.1186/s13014-018-1000-7.
[31] Janita E. van Timmeren, Madalyne Chamberlain, Jérôme Krayenbuehl, Lotte Wilke, Stefanie Ehrbar, Marta Bogowicz, Mariangela Zamburlini, Helena Garcia Schüler, Matea Pavic, Panagiotis Balermpas, Chaehee Ryu, Matthias Guckenberger, Nicolaus Andratschke, Stephanie Tanadini-Lang, "Comparison of beam segment versus full plan re-optimization in daily magnetic resonance imaging-guided online-adaptive radiotherapy," Physics and Imaging in Radiation Oncology, Volume 17, 2021, Pages 43-46.
[32] Böck M. On adaptation cost and tractability in robust adaptive radiation therapy optimization. Med Phys 2020 Jul;47:2791–804. https://doi.org/10.1002/mp.14167. Epub 2020 May 22 PMID: 32275778.
[33] Liu X, Liang Y, Zhu J, Yu G, Yu Y, Cao Q, et al. A fast online replanning algorithm based on intensity field projection for adaptive radiotherapy. Front Oncol 2020 Mar;3:287. https://doi.org/10.3389/fonc.2020.00287. PMID: 32195188 PMCID: PMC7063069.

Downloaded for Anonymous User (n/a) at Baptist Health South Florida Inc from ClinicalKey.com by Elsevier on May 10, 2024. For personal use only. No other uses without permission. Copyright ©2024. Elsevier Inc. All rights reserved.